Effect of Sb-doping on the morphology and the dielectric properties of chrysanthemum-like ZnO nanowire clusters*

Yan Jun-Feng(闫军锋), You Tian-Gui(游天桂), Zhang Zhi-Yong(张志勇)†,
Tian Jiang-Xiao(田江晓), Yun Jiang-Ni(贠江妮), and Zhao Wu(赵 武)

School of Information Science and Technology, Northwest University, Xi'an 710069, *China*

(Received 31 March 2012; revised manuscript received 9 May 2012)

Chrysanthemum-like ZnO nanowire clusters with different Sb-doping concentrations were prepared by using the hydrothermal process. The microstructures, morphologies, and dielectric properties of the as-prepared products were characterized by X-ray diffraction (XRD), high-resolution transmission electron microscopy (HRTEM), field emission environment scanning electron microscope (FEESEM), and microwave vector network analyzer respectively. The results indicate that the as-prepared products are Sb-doped ZnO single crystallines with hexagonal wurtzite structure, the flower bud saturation degree $F_{\rm d}$ is obviously different from that of the pure ZnO nanowire clusters, the good dielectric loss property is found in Sb-doped ZnO products with low density, and the dielectric loss tangent $\tan\delta_{\rm e}$ increases with the increase of the Sb-doping concentration in a certain concentration range.

Keywords: chrysanthemum-like ZnO nanowire clusters, dielectric properties, hydrothermal method, Sb doping

PACS: 80.10.Dn, 81.07.Gf, 81.16.–c, 77.22.Gm **DOI:** 10.1088/1674-1056/21/9/098001

1. Introduction

With the increasing use of gigahertz electromagnetic waves in industrial, commercial, and military applications, the electromagnetic pollution has become a serious problem and a matter of crucial concern recently.[1] Electromagnetic wave absorbing materials have attracted considerable attention and will play an important role in advanced electromagnetic wave shielding and stealth technology. However, the conventional electromagnetic wave absorbing materials could not meet the demands of strong absorption, wide frequency range, lightweight, and high resistivity. Therefore, it is urgent to develop new electromagnetic wave absorbing materials.[2]

It is well known that the nanostructured materials with unique chemical and physical properties can induce new mechanisms of electromagnetic loss and be used as electromagnetic wave absorbing and shielding materials.[3] With a wide direct bandgap, a large exciton binding energy, and rich morphologies, the nanostructured zinc oxide (ZnO) should be a good candidate for new absorbing materials due to its lightweight, high surface-to-volume ratio, and remarkable semiconductor properties.[4] The research groups of Zhou,[5] Cao,[6−9] Zhang,[10−12] Yan,[13,14] and Cao[15] have respectively made in-deep investigation on the electromagnetic wave absorption properties of the nanostructured ZnO with novel morphologies such as tetrapod-like ZnO whiskers, cagelike ZnO particles, ZnO nanowires, and ZnO nanotrees, and their research results have confirmed that ZnO is indeed a promising and vivid microwave absorbing material. Nevertheless, all those researches were focused on the pure ZnO, and most of the involved preparing methods needed high temperature and had low rates of products. In our previous work,[4,16,17] we fabricated chrysanthemum-like ZnO nanowire clusters with uniform morphology through the hydrothermal process at low temperature, and investigated the nucleation mechanism and the effect of polyacrylamide and Mn-doping on their morphologies and electromagnetic properties respectively.

In this paper, in order to improve the dielectric

*Project supported by the National Natural Science Foundation of China (Grant No. 60976069), the Natural Science Foundation of Shaanxi Province, China (Grant No. 2010JM6008), and the Xi'an Scientific and Technological Project, China (Grant No. CXY1008).

†Corresponding author. E-mail: Zhangzy@nwu.edu.cn

© 2012 Chinese Physical Society and IOP Publishing Ltd

property of the chrysanthemum-like ZnO nanowire clusters, we design and prepare some chrysanthemum-like Sb-doped ZnO nanowire clusters, and investigate the effect of Sb-doping on their morphologies and dielectric properties in details. The nanostructured ZnO product with good dielectric loss property and lightweight is obtained.

2. Experiment

In the experiment, the deionized water was used as the solvent, and an appropriate sodium hydroxide (NaOH) solution was added to the mixed liquid of zinc acetate dihydrate ($Zn(CH_3COO)_2{\cdot}2H_2O$) and antimony trichloride ($SbCl_3$), accompanied with a cold water bath and stirring, which formed a transparent and stable precursor. The final concentrations of the raw materials in the precursor are listed in Table 1. The precursor was then put into a Teflon-lined 50-mL-capacity autoclave, of which the compactedness was about 70%. After that, the autoclave was put into a bake oven with the temperature maintained at 200 °C for 12 h. Finally, the products were kept scoured and filtered until the PH value of the filtrate reached 7, and then dried at 60 °C in air for further characterization.

Table 1. Final concentrations of the raw materials in the precursor and the performance indexes of as-prepared products.

Sample	$[Zn^{2+}]$/mol·L^{-1}	$[OH^-]$/mol·L^{-1}	$[Sb^{3+}]/[Zn^{2+}]$	L_d	ρ/g·cm^{-3}
1	0.1	1.4	0	11.25	4.243
2	0.1	1.4	1%	9.98	1.085
3	0.1	1.4	3%	12.06	0.842
4	0.1	1.4	5%	10.13	1.070

The microstructures and the morphologies of the ZnO products were examined by X-ray diffraction (XRD, D/Max2550VB+/PC, Rigaku, Japan), high-resolution transmission electron microscopy (HRTEM, JEM-3010, JEOL, Japan), and field emission environment scanning electron microscope (FEESEM, Quanta 400 FEG, FEI, Holand) respectively. The ZnO particles/paraffin composites were prepared by dispersing the ZnO product with a weight ratio of 20% into a paraffin, which was transparent for the microwave, and the electromagnetic parameters of the composites in the X band (8.2–12.4 GHz) were measured by a microwave vector network analyzer (Agilent technologies E8362B, Agilent, America).

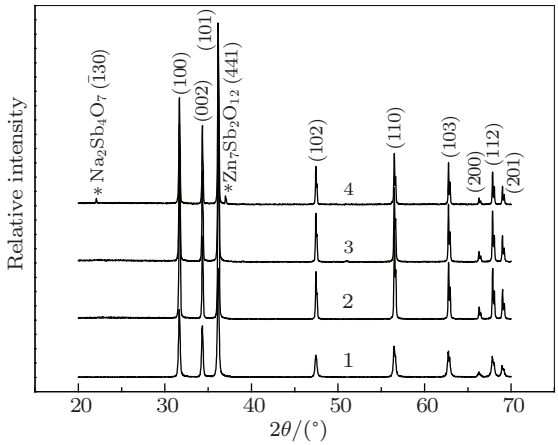


Fig. 1. XRD patterns of as-prepared ZnO products.

3. Results and discussion

3.1. XRD analysis

Figure 1 shows the XRD patterns of the as-prepared products with different Sb-doping concentrations. The major diffraction peaks can be indexed according to the hexagonal wurtzite structure ZnO (space group $p6_3mc$(186); JCPDS card No. 36-1451). There is no detectable secondary phase, except for $Na_2Sb_4O_7$ and $Zn_7Sb_2O_{12}$ in sample 4, which implies that the ratio of $[Sb^{3+}]$ to $[Zn^{2+}]$, i.e. 5%, is improper.

3.2. HRTEM analysis of as-prepared ZnO products

HRTEM images of the nanowires taken from the as-prepared ZnO products are shown in Fig. 2. Figure 2(a) shows a typical ZnO nanowire at 200 °C. The selected-area electron diffraction (SAED) pattern in Fig. 2(b) and the HRTEM image in Fig. 2(c) confirm that the ZnO nanowire is single crystalline with hexagonal wurtzite structure and space group $p6_3mc$ and the growth direction is along [0001].

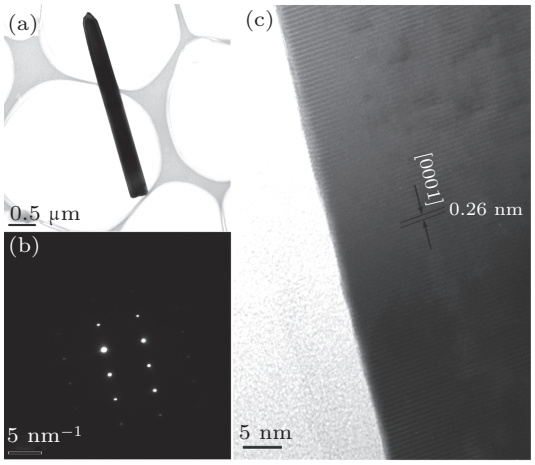


Fig. 2. (a) HRTEM image of a nanowire taken from the as-prepared ZnO products, (b) SAED image of the nanowire showing a [0001] growth direction, and (c) HRTEM image taken from the lateral surface of the nanowire in panel (a).

3.3. Effect of Sb-doping on the growth mechanism of as-prepared ZnO products

A group of SEM images of the as-prepared ZnO products, i.e., samples 1, 2, 3, and 4, are shown in Figs. 3(a)–3(d), in which the insets are the corresponding higher magnification SEM images. By analyzing Fig. 3, we find that all the as-prepared ZnO products with different Sb-doping concentrations have the uniform three-dimensional chrysanthemum-like structure but with different slenderness ratios[16,17] $L_{\rm d}$ listed in Table 1. To further study the chrysanthemum-like ZnO structure qualitatively, the flower bud saturation degree $F_{\rm d}$ defined as the quantity of the petal-like nanowires in the chrysanthemum-like structure, which reveals the flower bud saturation level of the chrysanthemum-like structure, is estimated roughly according to the SEM images. The larger the amount of nanowires in the chrysanthemum-like structure is, the larger the value of $F_{\rm d}$ is. Obviously, the $F_{\rm d}$ values of chrysanthemum-like ZnO nanowire clusters with Sb-doping are all less than that of the undoped as-prepared product and are almost equal to each other. Simultaneously, in order to verify the validity of the above quantitative and qualitative analysis, the densities of the as-prepared products, ρ, are measured and presented in Table 1. Moreover, almost all the nanowires have planar front tips except sample 1. It is noticeable that the Sb doping makes great influence on the growth habit of chrysanthemum-like ZnO nanowire clusters.

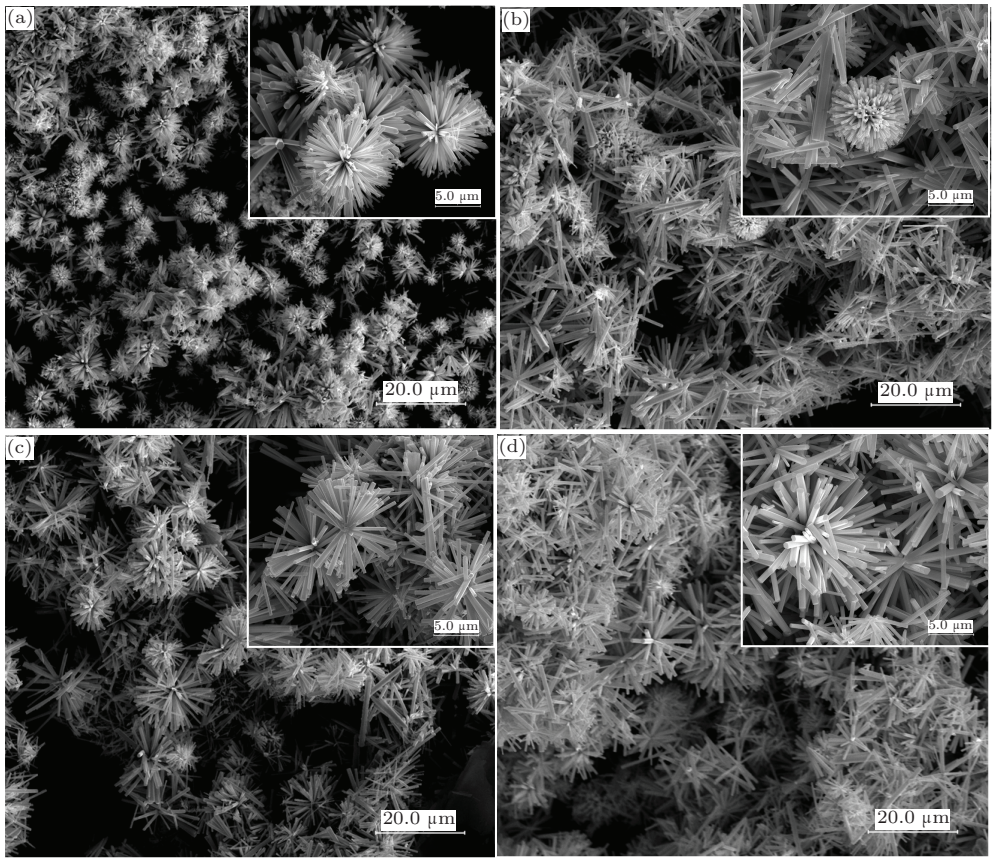


Fig. 3. FEESEM images of the as-prepared ZnO products: (a) sample 1, (b) sample 2, (c) sample 3, and (d) sample 4. The insets are the corresponding higher magnification images.

On the one hand, due to the Coulomb interaction, the Sb^{3+} ions from the ionization of doping agent could easily absorb on the basic cells of crystalline growth, $[Zn(OH)_4]^{2-}$, and act as the carriers, which may effectively improve $[Zn(OH)_4]^{2-}$ to fold together to form a ZnO crystal nucleus. Thus, the nucleation density increases only within certain limits under the synergistic constraints of supersaturation, reacting temperature, and systematical pressure. However, the quantity of nuclei slightly reduces in the multi-twin central nucleus due to the Coulomb repulsion from the nuclei absorbing a small number of Sb^{3+} ions, which results in the decrease of F_d radically. Under the adequate environmental driving force,[16] the c axes of the individual nucleus uniformly arranges along the radial direction of the sphere in a multi-twin central nucleus. Thus, the multi-twin central nuclei with special internal structures form and further develop to form chrysanthemum-like ZnO nanowire clusters. When the ratio of $[Sb^{3+}]$ to $[Zn^{2+}]$ varies from 0 to 5%, the quantity of petal-like nanowires in the chrysanthemum-like structure decreases due to the fact that the above Coulomb repulsion interaction enhances to a certain degree to form the situation shown in Fig. 3, and obviously F_d of sample 1 is the largest.

On the other hand, these multi-twin central nuclei further develop to form chrysanthemum-like ZnO nanowire clusters in a certain range of supersaturation. Above all, in the growth environment with Sb^{3+} and Cl^- ions, the (0001) preferential orientation of ZnO is still kept, while the growth rate of positive polar axial plane somewhat drops, and the way for the basic cells of crystalline growth $[Zn(OH)_4]^{2-}$ folding together to enter the crystal lattice space is changed from the step type to the layered type.[18] As a result, almost all the nanowires with the Sb^{3+} and Cl^- ions have planar front tips, while sample 1 presents a tapered front tip. Obviously, the Sb doping has a great influence on the growth habit of chrysanthemum-like ZnO nanowire clusters. When the ratio of $[Sb^{3+}]$ to $[Zn^{2+}]$ increases in the range from 1% to 3%, the basic cells of crystalline growth $[Zn(OH)_4]^{2-}$ folding together in the layered type along the (0001) direction is enhanced, and the L_d value increases. While the ratio of $[Sb^{3+}]$ to $[Zn^{2+}]$ reaches 5%, the smaller value of L_d in sample 4 may result from the secondary phases of $Na_2Sb_4O_7$ and $Zn_7Sb_2O_{12}$. The L_d difference between the undoped and the Sb-doped samples may derive from the different folding together types of the basic cells of crystalline growth. On the basis of the above analysis, it is easily concluded that the density ρ (see Table 1) differences of as-prepared products directly result from F_d and L_d. From Table 1, it is evident that the density of sample 1, ρ_1, is nearly four times as large as those of samples 2 and 4, and is about five times as large as that of sample 3. For samples 2, 3, and 4, although they possess similar F_d values, the L_d of sample 3 is the largest, and the L_d of sample 4 is somewhat larger than that of sample 2, so $\rho_3 < \rho_4 < \rho_2$. However, the F_d of sample 1 with a larger L_d is far larger than those of the others, which leads to its largest density value. In turn, the sequence of density, $\rho_3 < \rho_4 < \rho_2 < \rho_1$, further verifies the correctness of the above analysis.

3.4. Dielectric properties

Figures 4(a)–4(c) show the real part of permittivity ε', the imaginary part of permittivity ε'', and the dielectric loss tangent $\tan\delta_e$ of samples 1, 2, 3, and 4 in the X band, respectively. It is clear that the real parts of permittivity ε' of samples 1, 2, 3, and 4 are nearly invariable in the X band, but gradually increase in the sequence of samples 4, 2, 1, and 3. The values of ε'' and $\tan\delta_e$ show the same tendency, which first increase with the rise of Sb-doping concentration and peak at 3% Sb doping, then sharply drop to the bottom at 5% Sb doping.

The real part of permittivity ε', which is caused by the displacement polarization, largely depends on the crystalline quality of the ZnO product. The 5% Sb doping not only leads to the secondary phases of $Na_2Sb_4O_7$ and $Zn_7Sb_2O_{12}$ detected by XRD but also greatly breaks the ZnO crystalline structure, which hampers the displacement polarization. So the value of ε' of sample 4 is the smallest. The dielectric loss tangent $\tan\delta_e$, defined as the ratio of ε'' to ε', results from the phase lag of the dipole oscillation with respect to the applied electric field and the contribution from the finite conductivity of the ZnO products. According to Refs. [16] and [17], it is clear that the dielectric loss mechanism of the ZnO products consists of the turning-direction polarization of the electric dipole, the associated relaxation phenomenon, and the conducting network. An appropriate Sb doping enhances the concentration of current carriers in ZnO, which certainly increases the conductivity of ZnO. Due to the interstitial Sb^{3+} ions, the thermionic polarization appearing under the temperature perturbation and the applied electric field causes additional

energy loss. Therefore, the value of $\tan\delta_e$ increases with the rise of Sb-doping concentration. On the other hand, the largest value of L_d also leads to the largest $\tan\delta_e$ of sample 3 by forming the conducting network.[16,17] However, when the Sb-doping concentration is up to 5%, the secondary phases of $Na_2Sb_4O_7$ and $Zn_7Sb_2O_{12}$ are generated and become scattering centers to the current carriers, which not only decrease the conductivity of ZnO but also limit the turning-direction polarization. So sample 4 possesses the smallest $\tan\delta_e$.

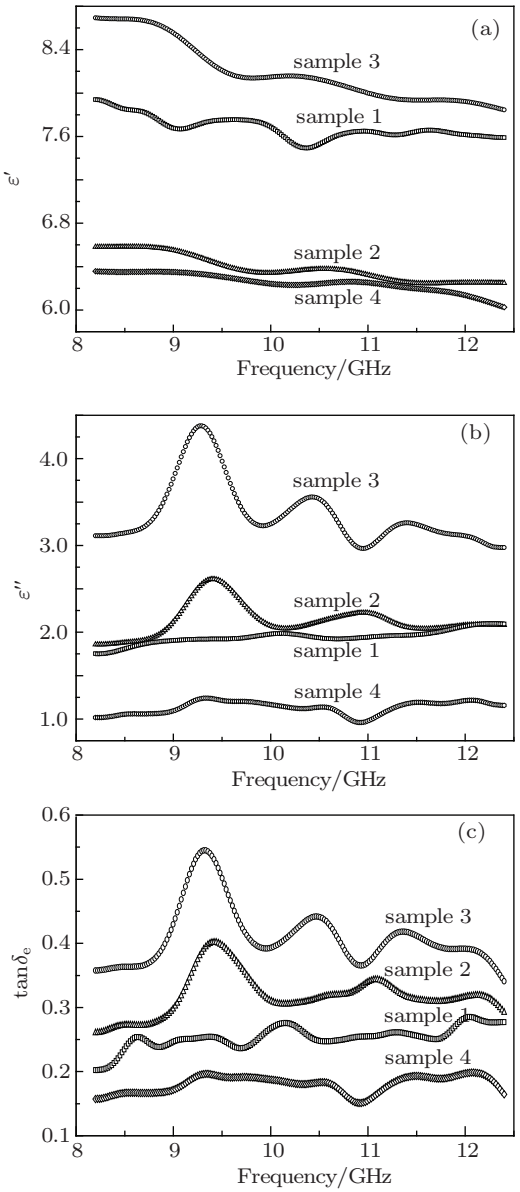


Fig. 4. (a) Real part of permittivity ε', (b) imaginary part of permittivity ε'', and (c) dielectric loss tangent $\tan\delta_e$.

4. Summary

Chrysanthemum-like ZnO nanowire clusters with different Sb-doping concentrations were prepared by using the hydrothermal process. Their microstructures, morphologies, and dielectric properties have been characterized. The Sb doping greatly changes the growth habit of chrysanthemum-like ZnO nanowire clusters, which results in the low densities of the as-prepared products and boosts up the dielectric loss property of ZnO. The lowest density is 0.842 g/cm^3 and the dielectric loss maximize in the X band when the Sb-doping concentration is 3%. It suggests that the Sb doping can improve the electromagnetic wave absorption property of chrysanthemum-like ZnO nanowire clusters, which may be used in the design of high-performance and lightweight microwave absorption materials.

References

[1] Zhou R F, Qiao L, Feng H T, Chen J T, Yan D, Wu Z G and Yan P X 2008 *J. Appl. Phys.* **104** 094101

[2] Ghasemi A, Hossienpour A, Morisako A, Saatchi A and Salehi M 2006 *J. Magn. Magn. Mater.* **302** 429

[3] Chen Y J, Cao M S, Wang T H and Wan Q 2004 *Appl. Phys. Lett.* **84** 3367

[4] Yan J F, You T G, Zhang Z Y, Tian J X, Yun J N and Zhao W 2011 *Chin. Phys.* B **20** 048102

[5] Zhou Z W, Chu L S and Hu S C 2006 *Mater. Sci. Eng.* B **126** 93

[6] Cao M S, Shi X L, Fang X Y, Jin H B, Hou Z L, Zhou W and Chen Y J 2007 *Appl. Phys. Lett.* **91** 203110

[7] Shi X L, Yuan J, Zhou W, Rong J L and Cao M S 2007 *Chin. Phys. Lett.* **24** 2994

[8] Zhou Y, Shi X L, Yuan J, Fang X Y and Cao M S 2007 *Chin. Phys. Lett.* **24** 3264

[9] Huang Y Q, Yuan J, Song W L, Wen B, Fang X Y and Cao M S 2010 *Chin. Phys. Lett.* **27** 027702

[10] Cao J W, Huang Y H, Zhang Y, Liao Q L and Deng Z Q 2008 *Acta Phys. Sin.* **57** 3641 (in Chinese)

[11] Li H F, Huang Y H, Sun G B, Yan X Q, Yang Y, Wang J and Zhang Y 2010 *J. Phys. Chem.* C **114** 10088

[12] Wang J, Li H F, Huang Y H, Yu H B and Zhang Y 2010 *Acta Phys. Sin.* **59** 1946 (in Chinese)

[13] Zhuo R F, Feng H T, Chen J T, Yan D, Feng J J, Li H J, Geng B S, Cheng S, Xu X Y and Yan P X 2008 *J. Phys. Chem.* C **112** 11767

[14] Zhou R F, Feng H T, Liang Q, Liu J Z, Chen J T, Yan D, Feng J J, Li H J, Cheng S, Geng B S, Xu X Y, Wang J, Wu Z G, Yan P X and Yue G H 2008 *J. Phys.* D: *Appl. Phys.* **41** 185405

[15] Huang Y X, Cao Q X, Li Z M, Jiang H Q, Wang Y P and Li G F 2009 *J. Am. Ceram. Soc.* **92** 2129

[16] Yan J F, Zhang Z Y, You T G, Zhao W and Yun J N 2009 *Chin. Phys.* B **18** 4019

[17] Yan J F, Zhang Z Y, You T G, Zhao W, Yun J N and Zhang F C 2009 *Chin. Phys.* B **18** 4552

[18] Zhang K C and Zhang L H 1997 *Crystal Growth Science and Technology* (Beijing: Science Press) p. 92 (in Chinese)